High-Precision Benchmarks for the Stochastic Rod

Eugene d'Eon,[*,a] and Anil Prinja[b]

[a] *NVIDIA*
2788 San Tomas Expressway, Santa Clara, CA 95050
ORCID: 0000-0002-3761-2989

[b] *University of New Mexico*
Department of Nuclear Engineering, Albuquerque, NM 87131

[*]Email: ejdeon@gmail.com

Number of pages: 23
Number of tables: 4
Number of figures: 4

Abstract

We demonstrate a method to calculate high-precision benchmarks for the reflectance and transmittance of a finite rod with a stochastic cross section, assuming that the attenuation law has a known closed form and both the single-scattering albedo and scattering kernel are deterministic. We introduce new 10-digit values for an existing binary-Markov benchmark (including mean and variance), along with several new benchmarks defined for non-Markov binary mixtures and a continuous fluctuation model featuring gamma stationary statistics. Furthermore, we reveal that our analysis of scattering in the stochastic rod enables a practical algorithm for identifying the parameters of an n-ary Markov mixture that most accurately approximates transport in a non-Markov system.

Keywords — Stochastic Media, Benchmark, Markov Mixture, Rod, CIR

I. INTRODUCTION

Stochastic descriptions of linear transport in media exhibiting complex spatial material property variation are widely employed in applications such as inertial confinement fusion, advanced nuclear reactors, and radiation transport in clumpy media [1, 2, 3]. Deterministic transport on a highly heterogeneous material domain is modeled by a transport equation with spatially random interaction cross-sections and the problem reduces to one of creating realizations of stochastic geometry, solving the transport equation on an ensemble of realizations, and post-processing the results to obtain quantities of interest, such as the mean radiation reflectance and transmittance as well as the interior flux [4, 5]. Although expensive to generate, these solutions provide important benchmarks against which to measure the accuracy of efficient approximate models of non-classical transport. Deterministic results, where possible, permit a more efficient exploration of stochastic transport and can lead to additional insights. However, exact deterministic results have been limited to purely-absorbing systems or one-dimensional, semi-infinite systems with deterministic single-scattering albedo [6, 7].

In this paper, we present a new exact analytic transport result for steady-state monoenergetic transport in a stochastic *finite* 1-D rod with scattering, provided the single-scattering albedo and scattering kernel are both deterministic and homogeneous. In particular, we solve the albedo problem for the finite rod and show that the ensemble-averaged reflectance R and transmittance T of a finite rod follow directly from the attenuation law of the system. We further extend the approach to compute the variances of R and T. Our approach is numerically stable and efficient, bypassing direct use of the density of optical depths. We use it to present the first, to our knowledge, deterministic confirmation of the ALP rod benchmarks [4], which we give to 10 places.

Our method applies to any system where the attenuation law is known exactly, and we also give results for n-ary Markov mixtures, non-Markov binary mixtures and systems with transformed Gaussian fluctuations. Our main result also inspires new methods for determining parameters of an n-ary Markov mixture that best approximates the full transport in a non-Markov system, and we share some promising results of approximating transport in media with continuous density fluctuations using n-ary Markov approximations. Not all stochastic media are best described using a discretely fluctuating cross section, and these new correspondences potentially extend the reach of efficient approximations such as the Chord Length Sampling (CLS) [8] and conditional point sampling (CoPS) [9].

In the next section, we derive our new solution of the stochastic-rod albedo problem before presenting new benchmark solutions in section III. Then in section IV, we demonstrate how to approximate non-Markov systems with n-ary Markov mixtures.

II. STOCHASTIC TRANSPORT IN A FINITE ROD

In this section, we derive new solutions for linear transport in a stochastic rod. Transport in a half rod with deterministic albedo and stochastic density has been well studied previously [6, 10, 11, 12]. Our primary contribution is a new practical recipe for arbitrary precision in the *finite* stochastic rod, subject to some limitations.

In a simplified one-dimensional "rod", transport is restricted to flow left and right along the x axis [13]. Collisions are governed by a total macroscopic cross section $\Sigma(x)$ and scattering is characterized using a "mean cosine" $-1 \leq g \leq 1$, where $(1+g)/2$ is the probability that the scattered direction is the same as the incoming direction. We will assume that the single-scattering albedo $0 < c \leq 1$ is constant. The angular fluxes in such a source-free system satisfy [14]

$$\pm \frac{\mathrm{d}\psi_\pm}{\mathrm{d}x} = -\Sigma(x)\psi_\pm(x) + \Sigma(x)\frac{c(1+g)}{2}\psi_\pm(x) + \Sigma(x)\frac{c(1-g)}{2}\psi_\mp(x). \tag{1}$$

For the albedo problem, we assume an inward, unit, deterministic source at $x = 0$ and seek the reflectance (R) and transmittance (T) for the rod of length a (where $x \in [0, a]$). For a realization with deterministic $\Sigma(x)$, the albedos are [14]

$$R(a) = \frac{c(1-g)}{2\kappa \coth(\kappa\tau(a)) + c(-g) - c + 2} \tag{2}$$

$$T(a) = \frac{\kappa}{\big(1 - c(g+1)/2\big)\sinh(\kappa\tau(a)) + \kappa\cosh(\kappa\tau(a))}, \tag{3}$$

where $\kappa \equiv \sqrt{(1-c)(1-cg)}$ is a diffusion constant and

$$\tau(x) = \int_0^x \Sigma(x')\,\mathrm{d}x' \tag{4}$$

is the optical depth at position x from the left boundary.

For the stochastic case, we consider stationary fluctuations of $\Sigma(x)$, and seek ensemble averages of the albedos $\langle R(a)\rangle$, $\langle T(a)\rangle$. If the density of optical depths $f_a(\tau)$ of the rod of length a is known, then the averages follow directly from the deterministic solutions [6], where the only stochastic quantity is τ, for example

$$\langle R(a)\rangle = \int_0^\infty R(a) f_a(\tau)\, \mathrm{d}\tau. \tag{5}$$

However, in practice, $f_a(\tau)$ is often not known in closed form (excluding the case of non-physical Gaussian fluctuations) and the required integrals are likely intractable. However, the related Laplace transform

$$T_s(x) \equiv \langle \mathrm{e}^{-\tau(x)s}\rangle, \quad s \geq 0, \tag{6}$$

is known in closed form for many fluctuation models, as this is simply the attenuation law in the purely absorbing rod where the extinction field $\Sigma(x)$ is scaled by a constant s. While the density of optical depths follows from Equation 6, it involves a numerically-problematic inverse transform, so instead we seek to transform the deterministic albedos into a form where we can apply Equation 6 directly. We demonstrate this next, treating the absorbing and non-absorbing cases separately.

II.A. With Absorption

For the absorbing rod, we observe that the deterministic albedos (Equations 2 and 3) can be transformed into a sum of exponentials of the optical depth. Applying the appropriate trignometric expansions, multiplying top and bottom by $\mathrm{e}^{-\tau(a)}$ and expanding the geometric series, we can write

$$R(a) = \frac{(1-\beta)c(1-g)}{4\kappa} \sum_{n=0}^{\infty} \beta^n \left(e^{-2n\kappa\tau(a)} - e^{-2(n+1)\kappa\tau(a)} \right), \tag{7}$$

$$T(a) = (1-\beta) \sum_{n=0}^{\infty} \beta^n e^{-\kappa(2n+1)\tau(a)}, \quad \beta \equiv \frac{-2+c+cg+2\kappa}{-2+c+cg-2\kappa}. \tag{8}$$

We can now ensemble average these albedos directly using Equation 6 to produce an infinite sum of scaled transmission laws

$$\langle R(a)\rangle = \frac{(1-\beta)c(1-g)}{4\kappa} \sum_{n=0}^{\infty} \beta^n \left(T_{2n\kappa}(a) - T_{2(n+1)\kappa}(a) \right), \tag{9}$$

$$\langle T(a)\rangle = (1-\beta) \sum_{n=0}^{\infty} \beta^n T_{\kappa(1+2n)}(a), \tag{10}$$

which we find to converge rapidly in practice and amenable to high-precision benchmark computation.

These results illustrate an interesting relationship between related, but not identical, scattering and purely-absorbing systems. For example, note how the mean transmission $\langle T(a)\rangle$ in the rod with scattering is given exactly as an infinite sum of mean transmittances $T_{\kappa(1+2n)}(a)$ for rods of the same length a, but with no scattering and with the cross sections scaled by integer multiples of the diffusion constant κ.

Eqs.(9 - 10) include a degenerate 0^0 for the case of perfectly forward scattering ($g = 1$) because $\beta = 0$. In this case, the mean albedos reduce to $R(a) = 0$ and $T(s) = T_{1-c}(a)$, and the latter result is identical to the known transect attenuation law for a chain of forward-scattering collisions along a transect in a stochastic medium [15].

II.A.1. Variances

The same approach can be used to compute the variances of R and T. Using a similar expansion of the squares of Eqs.(7-8), followed by ensemble averaging, we find

$$\mathrm{Var}(R) = \frac{(1-\beta)^2 c^2 (1-g)^2}{16\kappa^2}\left(1 + \sum_{n=1}^{\infty}(\beta-1)\beta^{n-2}(\beta+\beta n - n + 1)T_{2n\kappa}(a)\right) - \langle R(a)\rangle^2, \quad (11)$$

$$\mathrm{Var}(T) = (1-\beta)^2 \sum_{n=0}^{\infty}\beta^{n-1} n T_{2n\kappa}(a) - \langle T(a)\rangle^2. \quad (12)$$

Extending this approach to higher-order moments is straightforward.

II.A.2. Count-Conditional Albedos

Taking the Taylor expansion about $c = 0$ of the ensemble-averaged albedos (Eqs.(9-10)) yields the count-conditional albedos $\langle R_n(a)\rangle$ and $\langle T_n(a)\rangle$ [16], where $\langle R_n(a)\rangle$ is the mean probability of a particle escaping the rod of length a after experiencing exactly n collisions inside the rod. Expanding the first few orders, we find new universal relations for low-order scattering from the stochastic rod:

$$\langle R_0(a)\rangle = 0 \tag{13}$$

$$\langle R_1(a)\rangle = \frac{1}{4}c(1-g)(1-T_2(a)) \tag{14}$$

$$\langle R_2(a)\rangle = \frac{1}{4}c^2(1-g)\left((g+1)T_2^{(1,0)}(a) + \frac{1}{2}(g+1)(1-T_2(a))\right) \tag{15}$$

and

$$\langle T_0(a)\rangle = T_1(a) \tag{16}$$

$$\langle T_1(a)\rangle = -\frac{1}{2}c(g+1)T_1^{(1,0)}(a) \tag{17}$$

$$\langle T_2(a)\rangle = \frac{1}{16}c^2\left(2(g+1)^2T_1^{(2,0)}(a) - (g-1)^2\left(2T_1^{(1,0)}(a) + T_1(a) - T_3(a)\right)\right), \tag{18}$$

in terms of derivatives of the mean attenuation law (Equation 6), defined by

$$T_s^{(j,k)}(x) \equiv \frac{\partial^j}{\partial s^j}\frac{\partial^k}{\partial x^k}T_s(x). \tag{19}$$

These expressions further exemplify how observables in the scattering rod can be decomposed into a combination of purely-absorbing calculations. For example, Equation 14 gives the probability of reflecting from the rod after one collision in terms of an absorption calculation $T_2(a)$ for a rod of the same length, but with the cross sections doubled in each realization ($s = 2$).

II.B. No Absorption

The case of no absorption ($c = 1$) requires a unique approach. For the lossless rod, the deterministic reflectance $R(a)$ and transmittance $T(a)$ in a given realization with optical thickness $\tau(a)$ are [14]

$$R(a) = 1 - T(a), \tag{20}$$

$$T(a) = \frac{2}{2+(1-g)\tau(a)}. \tag{21}$$

If we write Equation 21 as a Laplace integral,

$$T(a) = \frac{2}{1-g}\int_0^\infty e^{\frac{2s}{g-1}} \mathrm{e}^{-s\tau}\,\mathrm{d}s. \tag{22}$$

then we have

$$\langle T(a)\rangle = \frac{2}{1-g}\int_0^\infty\int_0^\infty e^{\frac{2s}{g-1}} \mathrm{e}^{-s\tau} f_a(\tau)\,\mathrm{d}s\,\mathrm{d}\tau \tag{23}$$

$$= \frac{2}{1-g}\int_0^\infty e^{\frac{2s}{g-1}} T_s(a)\,\mathrm{d}s, \tag{24}$$

using Equation 6, assuming we can swap the integration order. This is convenient as a numerical method, as it avoids numerical issues inverting $T_s(x)$ to find f_a.

For higher-order moments of T, we note the general Laplace transform

$$\big(T(a)\big)^n = \left(\frac{2}{2+(1-g)\tau}\right)^n = \frac{2^n}{(1-g)^n\,(n-1)!}\int_0^\infty e^{\frac{2s}{g-1}} s^{n-1} e^{-s\tau}\,\mathrm{d}s, \tag{25}$$

which, after ensemble averaging, yields the transmittance moments

$$\langle T(a)^n\rangle = \frac{2^n}{(1-g)^n\,(n-1)!}\int_0^\infty e^{\frac{2s}{g-1}} s^{n-1} T_s(a)\,\mathrm{d}s. \tag{26}$$

III. BENCHMARKS

We now apply the derivations in the previous section to produce a number of new high-precision benchmarks for the finite stochastic rod.

III.A. Discrete Mixtures

Discrete fluctuations, where $\Sigma(x)$ takes on one of n values $\Sigma_j, j = 1, 2, \ldots n$, at any position x, form a useful class of stochastic media [17]. Laser light transport in mixed zones in Rayleigh-Taylor unstable interface regions in inertial confinement fusion pellets and solar radiation transport in atmospheres with clouds are notable applications where two or more immiscible fluids manifest as discrete stochastic material mixtures. Monte Carlo and deterministic numerical benchmark solutions have been developed for 1D alternating slabs with Markovian mixing statistics, i.e., exponentially distributed chord lengths in the two materials, and used to assess the accuracy of approximate closure-based homogenized transport models, the most prominent being the Levermore-Pomraning (LP) model. More recently, this work has been extended to an arbitrary number of materials, so-called n-ary Markov mixtures [18], and multi-dimensions [5, 19, 20].

III.A.1. Markov Mixtures

For n-ary *Markov* mixtures, the required Laplace transform $T_s(x)$ is always a sum of n exponentials and can be compactly expressed as a matrix exponential [21, Eqs.(20,21)]

$$T_s(x) = \boldsymbol{\pi} e^{(Q-sS)x} \mathbf{1}, \tag{27}$$

where S is a diagonal matrix with the cross sections Σ_j in each phase, $\mathbf{1} = (1, 1, \cdots, 1)^T$, $\boldsymbol{\pi}$ is the equilibrium distribution of initial phases (volume fractions occupied by phase j) and Q is a matrix of transition coefficients, where $Q_{ij}\,\mathrm{d}s$ is the probability of transitioning from phase i to phase j when traversing a small distance $\mathrm{d}s$. The general T_s result in Equation 27 seems to have first appeared in the study of Markov-Modulated Poisson Processes [22]. For the well-studied case of binary Markov mixtures, $T_1(x)$ is the Levermore-Pomraning attenuation law.

Since the general attenuation in Eq.(27) can be computed to arbitrary precision, we can efficiently compute high-precision benchmarks for scattering in the stochastic rod using the methods derived in Section II. It is interesting to note that, since $T_s(x)$ is always a sum of n exponentials, the albedos R and T are therefore exactly represented as a countable sum of exponentials for any n-ary Markov system.

We now give several benchmark results for binary mixtures. In Table I, we give exact benchmark values for the $c = 0.9$ configuration of the ALP benchmarks [4], which were originally determined using the quenched-disorder approach [23]. We were able to achieve 10-point accuracy when truncating the summations at 25 terms in a time of 10^{-6} seconds. We observed a reduction in error proportional to e^{-2n}, where n is the number of terms in the sum, and computation time proportional to n. Using Eqs.(11 - 12), we further extend the original ALP benchmark by including exact variances.

Next, using Equation 23 for the mean transmittance in the case of no absorption ($c = 1$), we extend the ALP benchmarks to the lossless case, providing exact values in Table II.

Case	a	$\langle R(a)\rangle$	ALP (R)	Var(R)	$\langle T(a)\rangle$	ALP (T)	Var(T)
1	0.1	0.0336085547	0.0332	0.0051070843	0.9567341180	0.9572	0.0087422019
	1.0	0.2120602879	0.2121	0.0251034404	0.7017300622	0.7017	0.0592783333
	10.0	0.5146120962	0.5146	0.0001554905	0.0558841381	0.0557	0.0039173836
2	0.1	0.0311855790	0.0310	0.0061086706	0.9592533739	0.9595	0.0106827605
	1.0	0.1171004102	0.1173	0.0263761356	0.8198111270	0.8194	0.0817529106
	10.0	0.4298316332	0.4301	0.0113727340	0.2663732364	0.2658	0.0744737180
3	0.1	0.0406033351	0.0407	0.0015544326	0.9494962649	0.9494	0.0024073095
	1.0	0.2150813235	0.2157	0.0342908636	0.6957070903	0.6948	0.0707881374
	10.0	0.4689446932	0.4688	0.0146380875	0.1510863382	0.1510	0.0654108812

TABLE I
Exact ALP benchmark values for the $c = 0.9$ configurations. The original MC values included for comparison (uncertainty for those values was not reported).

Case	a	$\langle T(a)\rangle$	Var(T)
1	0.1	0.9614593667	0.006853462
	1.0	0.7406900320	0.042814787
	10.0	0.1852212671	0.0042717562
2	0.1	0.9638923466	0.008314012
	1.0	0.8440465606	0.058670050
	10.0	0.3515139061	0.0617658987
3	0.1	0.9544332317	0.001958766
	1.0	0.7365742979	0.052559115
	10.0	0.2593041025	0.0514596072

TABLE II
Exact benchmark values for the $c = 1$ extension of the ALP benchmarks.

III.A.2. Non-Markov Binary Mixtures

To produce an exact benchmark for a system where the Markov assumption is not appropriate, we require a random Σ field where exact attenuation law is known. For a binary mixture where the chord lengths along a transect are given by an alternating renewal process, the required attenuation law is known in terms of its Laplace transform. We noted three independent derivations of this result in the literature [24, 25, 26], which we verified to be equivalent. For Erlang-distributed chord-length distributions, and other simple models, $\tilde{T}_s$ can be inverted and new high precision benchmarks can be computed using our approach.

We propose a new benchmark for a non-Markovian binary rod with deterministic albedo $c = 0.9$ and isotropic scattering $g = 0$. For the two phases in the binary mixture, we chose Erlang chord lengths with densities $p_1(x) = e^{-x}x$ and $p_2(x) = \frac{128}{243}e^{-4x/3}x^3$, respectively. We assigned cross sections $\Sigma_1 = 12/5$ and $\Sigma_2 = 1/15$ to each phase, respectively. Symbolic computation software such as MATHEMATICA can easily invert the necessary Laplace transform to find T_s, but this results in a very bulky expression. For reference, the resulting attenuation law for $s = 1$

a	$\langle R(a)\rangle$	Var(R)	$\langle T(a)\rangle$	Var(T)
0.1	0.0399669216	0.0019874411	0.9501496532	0.0031035130
1.0	0.2140827329	0.0306370583	0.6974850029	0.0666697986
10.0	0.5146520340	0.0002016091	0.0542852987	0.0040831262

TABLE III

Mean and variance of the rod albedos for our non-Markov binary benchmark.

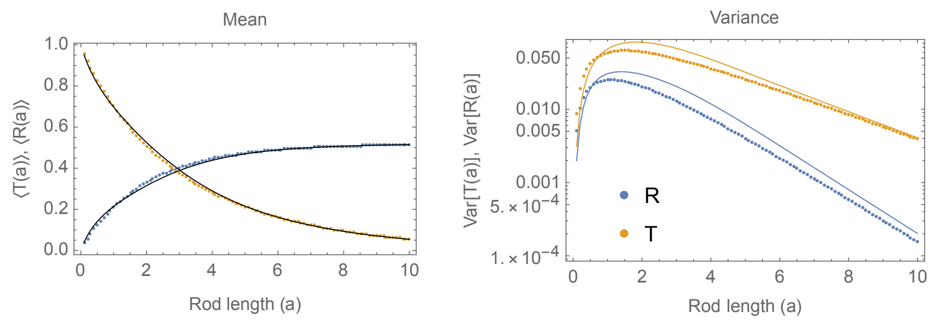

Fig. 1. Comparison of our non-Markov binary rod benchmark (continuous) to the ALP-Case-1 Markov benchmark (dots) as a function of rod length. Despite a close agreement of the mean albedos (left) over a range of rod lengths a, the non-Markov mixing statistics lead to a higher variance system for most rod lengths (right).

has Laplace transform:

$$\tilde{T}_1(p) = \frac{5\left(253125p^5 + 2885625p^4 + 12987000p^3 + 29429325p^2 + 34664145p + 18270604\right)}{\left(1125p^3 + 6975p^2 + 12915p + 5497\right)\left(1125p^3 + 6975p^2 + 12915p + 9497\right)}. \quad (28)$$

We provide reflectance and transmittance means and variances in Table III. We observed convergence to 10 places when truncating the sums in Eqs.(7-8) to 17 terms (and 25 terms for the variances).

The mixing parameters for this benchmark were intentionally chosen in order to closely match the *mean* albedos of the ALP Case 1 Markov $c = 0.9$ benchmark (Table I). In Figure 1, we compare both the mean and variance of the rod albedos between the two benchmarks as a function of rod length a. The figure shows that although the mean observables are well aligned over a range of system parameters, the variances are not as well aligned, clearly demonstrating the insufficiency of the mean for adequately characterizing the effects of stochasticity on physical quantities of interest. A large variance indicates that the system is inherently unpredictable and moment information is of limited value under these conditions. Extreme event probabilities such as the probability of exceeding threshold states are more meaningful in these situations, but clearly more challenging to compute.

III.B. TRANSFORMED-GAUSSIAN FLUCTUATIONS

Discrete fluctuations are not appropriate for every physical system. For radiation transport in turbulent plasmas and neutron transport in boiling water reactors and liquid-fueled molten salt reactors, for instance, random variation in the cross-section is more accurately characterized by continuous fluctuations. Gaussian stochastic processes in space and time are widely employed in this context [27, 10] but Gaussian fluctuations of Σ are problematic because negative values of the cross-section are admitted, which is nonphysical and leads to divergent solutions for the finite rod albedos. However, Gaussian processes can be used to drive fluctuations that give physically sound solution realizations. For instance, the Cox-Ingersoll-Ross (CIR) Cox process, which is a Poisson process driven by the sum of k squared Ornstein-Uhlenbeck (OU) processes, produces a $k/2$-gamma distributed stationary distribution for Σ. An example realization of two-dimensional CIR $k = 1$ noise is shown in Figure 3 (left). These non-negative continuous random fields are known as Feller processes [28], which are one of the six Pearson diffusions [29]. The Feller process offers a flexible family of continuous noises with known attenuation laws, and we use it now to present the first exact benchmark with scattering for a system with continuous fluctuations.

In the case of $k = 1$, corresponding to quadratic or squared-Gaussian statistics, the non-Markovian model can be embedded in a higher order Markovian process by driving the fluctuations with white noise Gaussian distributed stochastic $\eta(x)$ with mean $\langle \eta(x) \rangle = 0$ and correlation function $\langle \eta(x)\, \eta(x') \rangle = D\, \delta(x - x')$. The attenuation problem is then defined by the following pair of stochastic differential equations:

$$\frac{d}{dx}\tau(x) = \xi^2(x), \quad \tau(0) = 0, \tag{29a}$$

$$\frac{d}{dx}\xi(x) = -A\, \xi(x) + \eta(x), \quad \xi(0) = \xi_0, \tag{29b}$$

where the initial condition ξ_0 may be random or deterministic. The constants A and D are free parameters that can be used to appropriately scale the cross-section Σ. The joint process (τ, ξ) is Markovian with respect to the penetration distance x and, using standard manipulations of such stochastic differential equations [30], the associated joint probability density function $P(\tau, \xi, x)$ can be shown to satisfy the following Fokker-Planck equation (FPE):

$$\frac{\partial}{\partial x}P(\tau,\xi,x) = -\xi^2\,\frac{\partial}{\partial\tau}P(\tau,\xi,x) + A\,\frac{\partial}{\partial\xi}\left[\xi\,P(\tau,\xi,x)\right] + \frac{D}{2}\,\frac{\partial^2}{\partial\xi^2}P(\tau,\xi,x), \tag{30a}$$

$$P(\tau,\xi,0) = \delta(\tau)\,P_{\xi_0}(\xi_0). \tag{30b}$$

The ensemble-averaged attenuation then follows from

$$\langle \mathrm{e}^{-\tau(x)s}\rangle = \int_0^\infty d\xi \int_0^\infty e^{-s\tau}P(\tau,\xi,x)d\tau. \tag{31}$$

While a closed-form solution for the three dimensional (in τ,ξ,x) joint distribution appears intractable, ensemble averages with respect to τ satisfy reduced order FPEs that are solvable in certain instances. In particular, the partial ensemble average of the attenuation defined by

$$R(\xi,x) = \int_0^\infty e^{-s\tau}P(\tau,\xi,x)d\tau, \tag{32}$$

satisfies the lower-order equation FPE

$$\frac{\partial}{\partial x}R(\xi,x) = A\,\frac{\partial}{\partial\xi}\left[\xi\,R(\xi,x)\right] + \frac{D}{2}\,\frac{\partial^2}{\partial\xi^2}\left[R(\xi,x)\right] - \lambda\,\xi^2\,R(\xi,x), \tag{33}$$

while Equation (32) yields $\langle \mathrm{e}^{-\tau(x)s}\rangle = \int_0^\infty R(\xi,x)d\xi$. Equation (33) has been previously solved independently in a several different contexts and the general attenuation law is [31, 32]

$$T_s(x) = \left(\frac{e^{\frac{xy}{2}}}{\sqrt{\frac{\left(1-\frac{2\langle\Sigma\rangle s}{ky}\right)\sinh(\eta xy)}{\eta} + \cosh(\eta xy)}}\right)^k, \quad \eta = \sqrt{1-\frac{4\langle\Sigma\rangle s}{ky}}, \tag{34}$$

where the autocorrelation of the k independent OU processes is $R(|s-t|) = (\langle\Sigma\rangle/k)e^{-y|s-t|}$. Stochastic media with CIR Σ fluctuations and this attenuation law has been recently proposed for particle-laden turbulent flow [33].

a	$\langle R(a)\rangle$	Var(R)	$\langle T(a)\rangle$	Var(T)
0.1	0.0389587226	0.0023550422	0.9511991933	0.0038604858
1.0	0.1968964970	0.0262215535	0.7207973500	0.0641384161
10.0	0.4158252491	0.0199327259	0.2894548605	0.0925975274

TABLE IV
Mean and variance of the rod albedos for our CIR binary benchmark.

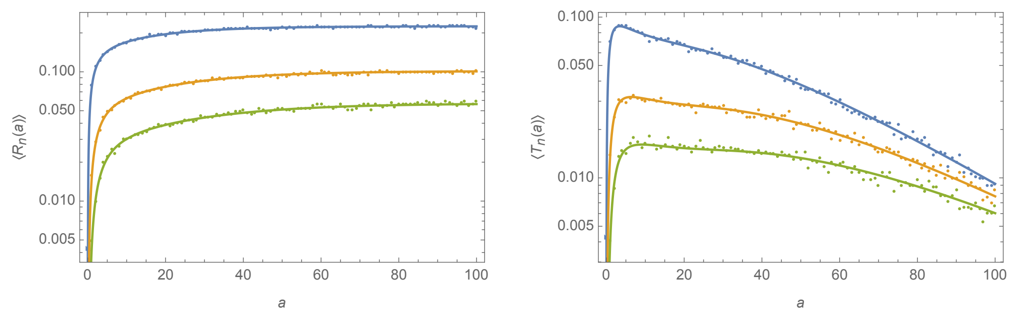

Fig. 2. Validation of Equation 14 etc. for the mean reflectance (left) and transmittance (right) after exactly n collisions: MC (dots) vs analytic (continuous) for $n \in \{1, 2, 3\}$. CIR fluctuations with $k = 1$, $y = 0.003$ and $\langle\Sigma\rangle = 0.3136$, isotropic scattering, $c = 0.9$.

III.B.1. A New Continuous-Fluctuation Benchmark

We define a CIR benchmark for the rod with $k = 1$, $y = 0.1$, $\langle\Sigma\rangle = 1$, $c = 0.9$, and isotropic scattering ($g = 0$). We provide reflectance and transmittance means and variances in Table IV. We observed convergence to 10 places when truncating the sums in Eqs.(7-8) to 17 terms (and 25 terms for the variances). Additionally, we validate the derivations for the n-th scattered albedos (subsubsection II.A.2) in Figure 2 by using quenched disorder (i.e. generating independent realizations of OU noise, squaring those values to determine $\Sigma(x)$ in the realization, and estimating the $R(n)$ and $T(n)$ in each using Woodcock tracking, and finally averaging many such results).

IV. MARKOV n-ARY APPROXIMATIONS

The efficiency of our approach permits a practical scheme for fitting Markov n-ary mixtures to a given non-Markov system. We present an initial investigation of this method here. Future work is required to more broadly explore the relationships between Markov and non-Markov systems in higher dimensions, possibly opening the door to applying methods such as Chord Length Sampling (CLS) and Conditional Point Sampling (CoPS) [34] to non-Markov systems.

In Section II, we showed that the mean and variance of the albedos of the rod are both purely a function of the scaled transmittance law $T_s(x)$. Therefore, it suffices to find n-ary mixture parameters that jointly minimize the loss of $T_s(x)$ over a range of values s and distances x. In practice, the Laplace inversions producing $T_s(x)$ for an n-ary Markov mixture involve root finding that challenges non-linear optimization routines. To circumvent this limitation, we note that the Laplace transform (with respect to x) of the n-ary attenuation law (Equation 27) is a simpler rational expression of s and p [22, Sec.2.4],

$$\tilde{T}_s(p) = \boldsymbol{\pi}(Ip - Q + sS)^{-1}\mathbf{1} \tag{35}$$

and so we jointly optimize for $\tilde{T}_s(p)$ over a range of s values and p values. We found that using integer multiples of the diffusion constant κ for s and uniform spacing of p works well in practice.

To demonstrate this approximation procedure, we approximated our CIR rod benchmark from the previous section using an n-ary Markov mixture with $n \in \{2, 3, 4, 5\}$. Following Hobson and Scheuer, we used a hierarchical transition matrix Q, as detailed in [21, Sec.3.2]. This reduced the number of variables to solve for in the approximation by requiring that the n phases adopt an increasing set of cross sections Σ_i and, additionally, that phase transitions are only permitted to the neighbouring phase(s). Figure 3 (right) illustrates how quantization of CIR noise tends to produce a discrete random field that satisfies this hierarchical property.

We used the FindFit procedure in Mathematica to fit the Laplace transforms in Eq.(35) to tabulated data of the target CIR system where s was the first 15 integer multiples of diffusion constant κ, and p was uniformly evaluated from 0 to 40 with dp $= 0.1$. For $n > 2$, we initially solved for parameters Σ_i and mean chord lengths Λ_i in a system constrained to exhibit equal volume fractions in each phase before relaxing the model to permit arbitrary volumes fractions. Beginning the more general optimization with the prior equal-volume-fraction initial conditions solved numerical issues in the optimization.

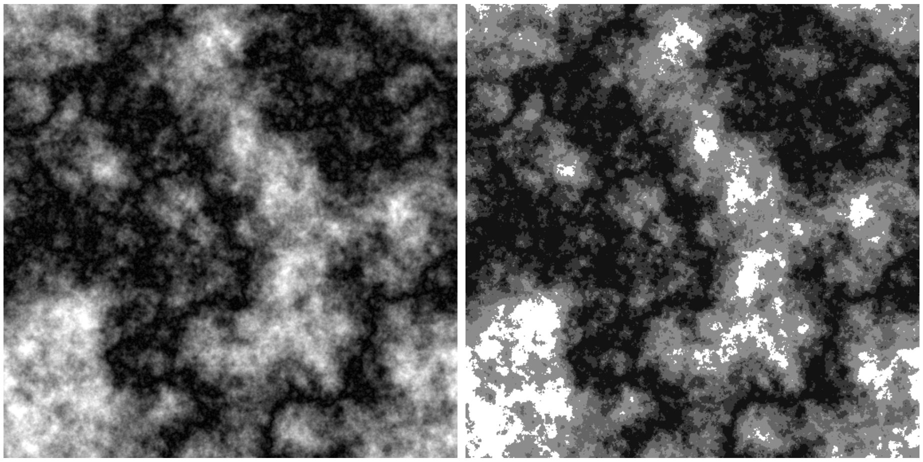

Fig. 3. Left: a two-dimensional realization of stationary CIR noise with $k = 1$. Right: An approximation of the random field on the left by quantizing the values into a 5-way discrete mixture using the solved parameters S_5 in this section. Notice how the quantized random field results in a hierarchical sequence of phase transitions along any transect: a transition to a phase 2 or more away is very unlikely.

For the four approximations of order n, we found the transition matrices Q_n to be:

$$Q_2 = \begin{pmatrix} -0.0279262 & 0.0279262 \\ 0.0232981 & -0.0232981 \end{pmatrix}, \quad Q_3 = \begin{pmatrix} -0.0637844 & 0.0637844 & 0 \\ 0.0528467 & -0.0734912 & 0.0206445 \\ 0 & 0.0220164 & -0.0220164 \end{pmatrix}$$

$$Q_4 = \begin{pmatrix} -0.130153 & 0.130153 & 0 & 0 \\ 0.133293 & -0.205295 & 0.0720022 & 0 \\ 0 & 0.051542 & -0.0635521 & 0.0120101 \\ 0 & 0 & 0.0173386 & -0.0173386 \end{pmatrix},$$

and

$$Q_5 = \begin{pmatrix} -0.175419 & 0.175419 & 0 & 0 & 0 \\ 0.175419 & -0.292094 & 0.116676 & 0 & 0 \\ 0 & 0.116676 & -0.196281 & 0.0796052 & 0 \\ 0 & 0 & 0.0796052 & -0.111067 & 0.031462 \\ 0 & 0 & 0 & 0.031462 & -0.031462 \end{pmatrix}.$$

The volume fractions that result from these Q matrices are, respectively,

$$\boldsymbol{\pi}_2 = \{0.454824, 0.545176\},$$
$$\boldsymbol{\pi}_3 = \{0.299516, 0.361506, 0.338978\},$$
$$\boldsymbol{\pi}_4 = \{0.233353, 0.227856, 0.318307, 0.220484\},$$
$$\boldsymbol{\pi}_5 = \{0.2, 0.2, 0.2, 0.2, 0.2\}.$$

We encountered numerical instabilities for the $n = 5$ optimization with arbitrary volume fractions and instead report the equal-volume-fractions result for $n = 5$.

The optimal cross sections (and mean cross sections $\langle\Sigma\rangle_n = S_n \cdot \boldsymbol{\pi}_n$) were found to be

$$S_2 = \{0.0733261, 1.30711\}, \qquad \langle\Sigma\rangle_2 = 0.745957, \quad (n = 2),$$
$$S_3 = \{0.0384934, 0.376838, 2.25165\}, \qquad \langle\Sigma\rangle_3 = 0.91102, \quad (n = 3),$$
$$S_4 = \{0.0215733, 0.200468, 0.739734, 3.06014\}, \qquad \langle\Sigma\rangle_4 = 0.960887, \quad (n = 4),$$
$$S_5 = \{0.0163243, 0.143596, 0.491551, 0.945288, 3.24069\}, \qquad \langle\Sigma\rangle_5 = 0.96749, \quad (n = 5),$$

where S_n form the S matrices in Eq. 27, consisting of Σ_i for the corresponding approximation order n.

The accuracy of these approximations for both the mean and variance of the albedos as a function of rod length is indicated in Figure 4. Note how all of the approximations do a reasonable job of fitting the mean albedos, but the mean accuracy improves and the variance greatly improves as the number of phases in the approximation is increased.

V. CONCLUSION

We have presented an efficient framework for computing high-precision albedos for stochastic finite rods, and used this to derive new benchmarks, which include binary Markov mixtures and a non-Markov binary mixture with Erlang-distributed chord lengths. Moreover, we have introduced the first exact benchmark for a scattering system with continuous fluctuations, using the Cox-Ingersoll-Ross process to model the cross-section fluctuations.

Additionally, we have investigated the approximation of non-Markov systems by n-ary Markov

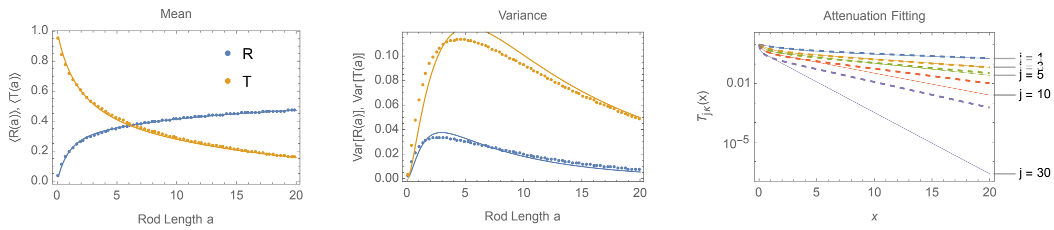

(a) Binary Markov approximation

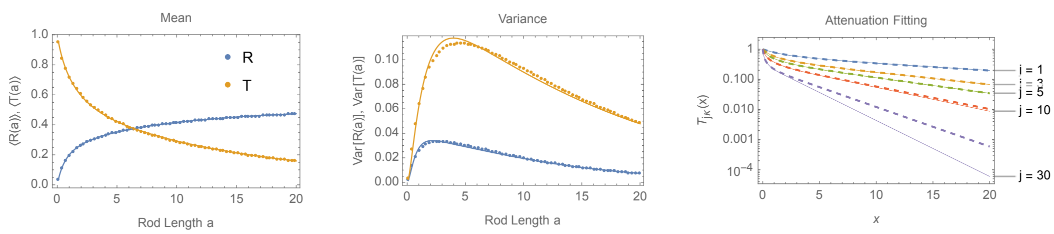

(b) 3-way Markov approximation

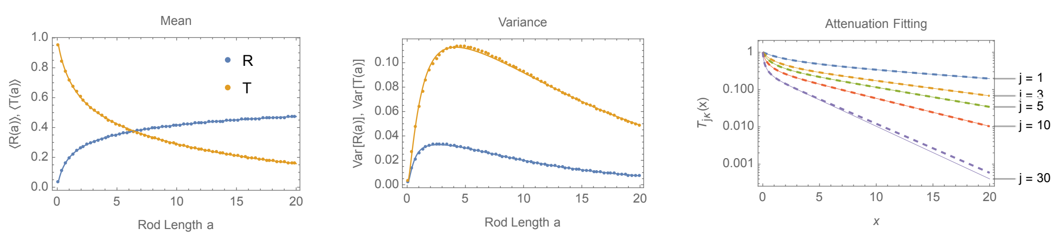

(c) 4-way Markov approximation

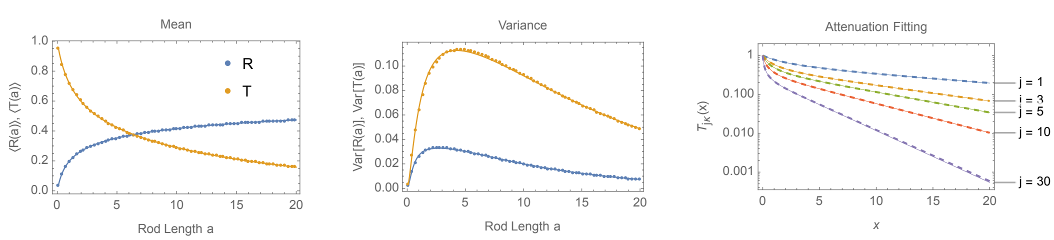

(d) 5-way Markov approximation

Fig. 4. Accuracy of n-ary approximations to our CIR benchmark. The left and middle plots indicate the accuracy of the approximation (continuous) to the reference data (dots) as a function of rod length. The right plots compare the accuracy of the fitted attenuation laws $T_{j\kappa}(x)$ for selected values of j (approximate model using dashed).

mixtures, which holds potential for enabling the application of efficient methods like Chord Length Sampling and Conditional Point Sampling to non-Markov systems. Our initial exploration demonstrates the feasibility of this approach, although further research is required to establish a more comprehensive understanding of the relationships between Markov and non-Markov systems.

In conclusion, the methods presented in this paper provide a foundation for more accurate and efficient analysis of radiative transport in stochastic media. By establishing reliable benchmarks and exploring the approximation of non-Markov systems by Markov mixtures, our work contributes to the development of new techniques and insights that can help advance the understanding of complex stochastic linear transport processes in various physical systems.

REFERENCES

[1] M. M. R. Williams, *Random processes in nuclear reactors*, Pergamon Press (1974).

[2] P. Boissé, "Radiative transfer inside clumpy media-The penetration of UV photons inside molecular clouds," *Astronomy and Astrophysics*, **228**, 483 (1990)URL http://adsabs.harvard.edu/abs/1990A%26A...228..483B.

[3] J. Kirk, "A theoretical analysis of the contribution of algal cells to the attenuation of light within natural waters I. General treatment of suspensions of pigmented cells," *New phytologist*, **75**, *1*, 11 (1975)URL https://doi.org/10.1111/j.1469-8137.1975.tb01366.x.

[4] M. Adams, E. Larsen, and G. Pomraning, "Benchmark results for particle transport in a binary Markov statistical medium," *Journal of Quantitative Spectroscopy and Radiative Transfer*, **42**, *4*, 253 (1989)URL https://doi.org/10.1016/0022-4073(89)90072-1.

[5] C. Larmier, F.-X. Hugot, F. Malvagi, A. Mazzolo, and A. Zoia, "Benchmark solutions for transport in d-dimensional Markov binary mixtures," *Journal of Quantitative Spectroscopy and Radiative Transfer*, **189**, 133 (2017)URL https://doi.org/10.1016/j.jqsrt.2016.11.015.

[6] G. Pomraning, "Classic transport problems in binary homogeneous Markov statistical mixtures," *Transport Theory and Statistical Physics*, **17**, *5-6*, 595 (1988)URL https://doi.org/10.1080/00411458808230878.

[7] E. W. Larsen and A. K. Prinja, "A new derivation of Akcasu's "MLP" equations for 1-D particle transport in stochastic media," *Annals of Nuclear Energy*, **35**, *4*, 620 (2008)URL https://doi.org/10.1016/j.anucene.2007.08.008.

[8] C. Larmier, A. Lam, P. Brantley, F. Malvagi, T. Palmer, and A. Zoia, "Monte Carlo chord length sampling for d-dimensional Markov binary mixtures," *Journal of Quantitative Spectroscopy and Radiative Transfer*, **204**, 256 (2018)URL https://doi.org/10.1016/j.jqsrt.2017.09.014.

[9] E. H. Vu and A. J. Olson, "Conditional Point Sampling: A Stochastic Media Transport Algorithm with Full Geometric Sampling Memory," *Journal of Quantitative Spectroscopy and Radiative Transfer*, 107767 (2021)URL https://doi.org/10.1016/j.jqsrt.2021.107767.

[10] A. K. Prinja and A. Gonzalez-Aller, "Particle transport in the presence of parametric noise," *Nuclear science and engineering*, **124**, *1*, 89 (1996)URL https://doi.org/10.13182/NSE124-89.

[11] A. Valentyuk, "A functional descripti stochastic radiative transfer," *Journal of Quantitative Spectroscopy and Radiative Transfer*, **56**, *3*, 447 (1996)URL https://doi.org/10.1016/0022-4073(96)84533-X.

[12] M. Selim and V. Bezák, "Rightfulness of summation cut-offs in the albedo problem with Gaussian fluctuations of the density of scatterers," *Czechoslovak journal of physics*, **53**, *6*, 449 (2003)URL http://doi.acm.org/10.1023/A:1024699907910.

[13] J. Hoogenboom, "The Two-Direction Neutral-Particle Transport Model: A Useful Tool for Research and Education," *Transport Theory and Statistical Physics*, **37**, *1*, 65 (2008)URL https://doi.org/10.1080/00411450802271791.

[14] G. Wing, *An introduction to transport theory*, Wiley (1962).

[15] E. d'Eon, "Beyond Renewal Approximations: A 1D Point Process Approach to Linear Transport in Stochastic Media," *ANS M&C 2023 - The international conference on Mathematics and Computational Methods Applied to Nuclear Science and Engineering - Niagara Falls, Ontario, Canada, Aug.* (2023).

[16] V. Ambartsumian, "On the number of scatterings by photon diffusion in turbid media," *Dokl AN Arm SSR*, vol. 8, 101–104 (1948).

[17] G. C. Pomraning, *Linear kinetic theory and particle transport in stochastic mixtures*, vol. 7, World Scientific (1991)URL https://doi.org/10.1142/1549.

[18] E. H. Vu, P. S. Brantley, A. J. Olson, and B. C. Kiedrowski1, "Benchmark comparisons of Monte Carlo algorithms for one-dimensional n-ary stochastic media," *ANS M&C 2021 - The international conference on Mathematics and Computational Methods Applied to Nuclear Science and Engineering - Raleigh, North Carolina, Oct.* (2021).

[19] A. Olson, S. Pautz, D. Bolintineanu, and E. Vu, "Theory and generation methods for N-ary stochastic mixtures with Markovian mixing statistics," *ANS M&C 2021 - The international conference on Mathematics and Computational Methods Applied to Nuclear Science and Engineering - Raleigh, North Carolina, Oct.* (2021).

[20] M. A. Kowalski, C. Larmier, and A. Zoia, "Analysis of heterogeneous Markov media for particle transport problems," *Physical Review E*, **106**, *4*, 044108 (2022)URL https://doi.org/10.1103/PhysRevE.106.044108.

[21] M. Hobson and P. Scheuer, "Radiative transfer in a clumpy medium–I. Analytical Markov-process solution for an N-phase slab," *Monthly Notices of the Royal Astronomical Society*, **264**, *1*, 145 (1993)URL https://doi.org/10.1093/mnras/264.1.145.

[22] W. Fischer and K. Meier-Hellstern, "The Markov-modulated Poisson process (MMPP) cookbook," *Performance evaluation*, **18**, *2*, 149 (1993)URL https://doi.org/10.1016/0166-5316(93)90035-S.

[23] G. Mikhailov, "Monte Carlo methods for solving problems with stochastic parameters," *Russian Journal of Numerical Analysis and Mathematical Modelling*, **2**, *2*, 137 (1987)URL https://doi.org/10.1515/rnam.1987.2.2.137.

[24] A. Lawrance, "Some models for stationary series of univariate events," P. A. W. Lewis (Editor), *Stochastic Point Processes: Statistical Analysis, Theory, and Applications*, 199–256, Wiley-Inter-science, New YorkURL https://www.researchgate.net/profile/Anthony_Lawrance/publication/260596754_Some_models_for_stationary_series_of_univariate_events/links/00b7d531b68c742c0c000000.pdf.

[25] D. Vanderhaegen, "Impact of a mixing structure on radiative transfer in random media," *Journal of Quantitative Spectroscopy and Radiative Transfer*, **39**, *4*, 333 (1988)URL https://doi.org/10.1016/0022-4073(88)90009-X.

[26] C. Levermore, J. Wong, and G. Pomraning, "Renewal theory for transport processes in binary statistical mixtures," *Journal of mathematical physics*, **29**, *4*, 995 (1988)URL https://doi.org/10.1063/1.527997.

[27] A. PRINJA, "Transport in random media with space-time noise," *Progress in Nuclear Energy*, **30**, *3*, 287 (1996)URL https://doi.org/10.1016/0149-1970(95)00090-9.

[28] W. FELLER, "Two singular diffusion problems," *Annals of mathematics*, **54**, *1*, 173 (1951)URL https://doi.org/10.2307/1969318.

[29] J. L. FORMAN and M. SØRENSEN, "The Pearson diffusions: A class of statistically tractable diffusion processes," *Scandinavian Journal of Statistics*, **35**, *3*, 438 (2008)URL https://doi.org/10.1111/j.1467-9469.2007.00592.x.

[30] C. W. GARDINER, *Handbook of stochastic methods for physics, chemistry and the natural sciences*, Springer (1985).

[31] A. SIEGERT, "A systematic approach to a class of problems in the theory of noise and other random phenomena–II: Examples," *IRE Transactions on Information Theory*, **3**, *1*, 38 (1957)URL https://doi.org/10.1109/TIT.1957.1057391.

[32] G. BÉDARD, "Photon counting statistics of Gaussian light," *Physical Review*, **151**, *4*, 1038 (1966)URL https://doi.org/10.1103/PhysRev.151.1038.

[33] A. J. BANKO, L. VILLAFANE, J. H. KIM, M. ESMAILY, and J. K. EATON, "Stochastic Modeling of Direct Radiation Transmission in Particle-Laden Turbulent Flow," *Journal of Quantitative Spectroscopy and Radiative Transfer* (2019)URL https://doi.org/10.1016/j.jqsrt.2019.01.005.

[34] E. H. VU and A. J. OLSON, "A Limited-Memory Framework for Conditional Point Sampling for Radiation Transport in 1D Stochastic Media," *Nuclear Science and Engineering*, **197**, *2*, 212 (2023)URL https://doi.org/10.1080/00295639.2022.2116378.